Journal of Biomedical Optics 9(3), 624–631 (May/June 2004)

Optical characterization of bovine retinal tissues

Dhiraj K. Sardar
Felipe S. Salinas
John J. Perez
Department of Physics and Astronomy
The University of Texas at San Antonio
San Antonio, Texas 78249-0697

Andrew T. C. Tsin
Department of Biology
The University of Texas at San Antonio
San Antonio, Texas 78249-0662

Abstract. An in-depth characterization of the optical properties of bovine retinal and retinal pigment epithelium-choroidal tissues has been performed. The indices of refraction of these ocular tissues were determined by applying Brewster's law. The inverse adding doubling method based on the diffusion approximation and radiative transport theory is applied to the measured values of the total diffuse transmission, total diffuse reflection, and collimated transmission to calculate the optical absorption, scattering, and scattering anisotropy coefficients of the bovine retinal and retinal pigment epithelium-choroidal tissues. The values of the optical properties obtained from the inverse adding doubling method are compared with those generated by the Monte Carlo simulation technique. Optical polarization measurements are also performed on bovine retinal tissues. Our studies show that both retina and retinal pigment epithelium-choroid possess strong polarization characteristics. [DOI: 10.1117/1.1688813]

Keywords: lasers, retinal tissues, optical properties, polarization.

Paper 02071 received Oct. 16, 2002; revised manuscript received May 19, 2003; accepted for publication Aug. 29, 2003.

1 Introduction

Although there have been some studies on ocular melanin,[1,2] a systematic investigation of the optical properties of intact ocular tissues is lacking. In this article, we present an in-depth characterization of the optical properties of bovine retinal and retinal pigment epithelium (RPE)-choroidal tissues. Melanin, a dark-brown pigment abundantly present in human skin, RPE, and choroid, is one of the primary biological components for light absorption and scattering. The chemical composition of melanin may be described as sulfur-containing (pheomelanin) or sulfur free (eumelanin), although most physiological melanins consist of two types of copolymer.[1] Dryja et al.[3] have shown that the melanin in RPE and choroid is similar, with a low sulfur content of approximately 1%, indicating a largely eumelanin composition. The optical properties, however, do not differ significantly between eumelanin and pheomelanin. Melanin in the RPE and choroidal tissues strongly absorbs the higher energy photons of ultraviolet radiation, which are very phototoxic to the human eye. It is also believed that melanin-rich skin has a natural resistance to skin cancer induced by solar exposure. A recent study by Sardar et al.[2] has shown that the scattering is predominant over the absorption in melanin prepared from melanosomes isolated from bovine RPE.

Biological materials (e.g., tissue and blood) are found to strongly scatter light.[4,5] Mourant et al.[4] have demonstrated that the light-scattering property of biomaterials can be used as a diagnostic means for determining tissue pathology.[4] Since medical laser applications for ocular diseases have steadily increased over the past several years and have become more complex, it is imperative that we understand the fundamental optical properties of ocular tissues because they influence the distribution and propagation of light in laser-irradiated tissues. Owing to the complex nature of retinal and RPE-choroidal tissues, both their absorption and scattering properties must be considered for medical applications of lasers.

The quantitative distribution of light intensity in biological media can be obtained from the solution of the radiative transport equation.[6] The details of this equation and the application of the Henyey-Greenstein scattering approximation to biological media can be found in Ref. 2. Although the transport equation is difficult to solve analytically for biological media because of the inherent inhomogeneities and irregularities in their physical shapes, an approximate solution can be obtained by assuming homogeneity and regular geometry of the medium, and thus an estimate of light intensity distribution can be obtained by solving the radiative transport equation. In order to do this, the values for the absorption, scattering, and scattering anisotropy coefficients are needed. Therefore, an appropriate experimental method is necessary to measure these fundamental optical properties.

Although a single measurement of the total transmission through a sample of known thickness provides an attenuation coefficient for Beer's law of exponential decay, it is impossible to separate the attenuation that is due to absorption from the loss that is due to scattering. This problem, to some extent, has been resolved by the one-dimensional, two-flux Kubelka-Munk model,[7] which has been widely used to determine the absorption and scattering coefficients of biological media,[8–13] provided the scattering is significantly dominant over the absorption. This model provides simple mathematical expressions for determining the optical parameters from the diffuse reflection and transmission measurements. In the past, researchers have applied the diffusion approximation to the transport equation to study biological media.[14–16] Most nota-

Address all correspondence to Dhiraj K. Sardar, Department of Physics and Astronomy, The University of Texas at San Antonio, San Antonio, TX 78249-0697. Tel: 210-458-5748; E-mail: dsardar@utsa.edu

1083-3668/2004/$15.00 © 2004 SPIE

bly, following the Kubelka-Munk model and diffusion approximation, an excellent experimental method was described by Van Gemert et al.[17] and Van Gemert and Star[18] for determining the absorption and scattering coefficients and the scattering anisotropy factor.

Even though the general solution is not available, an elaborate numerical solution is possible using the Monte Carlo (MC) simulation technique.[19–21] An important numerical approach known as the inverse adding doubling (IAD) method has been employed to solve the transport equation.[22] Both the IAD method and MC simulation technique provide more accurate estimates of optical properties for turbid media than any other models previously used. The details of the IAD method can be found in Ref. 2.

Retinal and RPE-choroidal tissues are found to be inherently birefringent and thereby possess an important optical polarization property. Based on their geometry and optical characteristics, these tissues have the intrinsic property of altering the polarization of incident light in every scattering event. Therefore, in addition to characterizing fundamental optical properties, polarization measurements have also been made for bovine retinal and RPE-choroidal tissues.

2 Materials and Methods

2.1 *Retinal and RPE-Choroidal Tissue Preparation*

Samples of retinal and RPE-choroidal tissues were prepared from fresh bovine eyes (left and right) obtained from local slaughter plants; the eyes were preserved on ice and transported to our laboratory in less than an hour. Upon arrival in the laboratory, anterior segments, including cornea, lens, and aqueous vitreous humor fluid, were removed from the eyes. The retina was then carefully lifted from the posterior eye cup and mounted between two glass slides. The RPE-choroid was subsequently removed from the eye and similarly mounted. The thicknesses of the retinal and RPE-choroidal tissues were approximately 0.15 and 0.10 mm, respectively. A small amount of vacuum grease was applied to the edges of the glass slides in order to maintain the moisture of the tissue sample. All of the data were collected at room temperature within 2 h from the slaughter of the animals.

2.2 *Measurement of Index of Refraction*

The indices of refraction of the retinal and RPE-choroidal tissues were determined by using Brewster's law.[23] According to this law, the index of refraction (n) of the tissue can be determined by the following expression:

$$\tan \theta_p = n, \tag{1}$$

where θ_p is the polarizing angle or Brewster's angle of incidence, which is achieved only when the refracted and reflected beams at the sample surface are at right angles; then the reflected beam would be 100% polarized. The index of refraction of air is taken to be 1. Under these circumstances, for an incoming unpolarized wave made up of two incoherent orthogonal p-states (i.e., linearly polarized or plane polarized), only the component that is polarized normal to the incident plane and therefore parallel to the surface will be reflected. Using the combination of a xenon arc lamp and a monochromator, a beam of unpolarized light at a known wavelength was directed onto the ocular tissue sample retained in between glass slides and mounted vertically on a calibrated table. The polarizing angle θ_p was found by using a linear polarizing analyzer; the index of refraction was calculated for that particular wavelength using Eq. (1). This measurement was repeated for four different wavelengths (450, 500, 550, and 600 nm) selected through the monochromator.

2.3 *Measurement of Scattering Anisotropy*

Using an independent experimental technique, the scattering anisotropy coefficient g can also be obtained from the measurements of scattered light intensities (I) at various scattering angles (θ) using a goniometer table. The scattering anisotropy coefficient g is given by the average cosine of the scattering angle θ according to Eq. (2):

$$g = \frac{\Sigma_i (\cos \theta_i) I_i}{\Sigma_i I_i}, \tag{2}$$

where the sums are taken over all values (i) of the scattering angles and intensities. The scattering anisotropy coefficient was obtained by irradiating the individual ocular tissue sample with a helium:neon (He:Ne) laser. The sample was placed in the sample holder affixed to the center of the goniometer table. The measurements were taken using an Oriel (model 77341) photomultiplier tube (PMT) mounted at the edge of the table. The PMT was powered by a Bertan (model 215) power supply. The He:Ne laser beam was aligned at a right angle with respect to the plane of the tissue sample, and the PMT was attached to an adjustable pointer that could be rotated around the circular goniometer table for measuring the scattered intensities at different angles. The scattered light intensity was measured between 0 and 180 deg at increments of 1 deg from 0 to 10 deg of scattering angle, and increments of 5 deg above 10 deg of scattering angle. Further experimental details can be found in Ref. 2.

2.4 *Measurement of Diffuse Reflectance and Transmittance*

Total diffuse reflectance and total diffuse transmittance were measured using the two identical integrating spheres (Oriel model 70451). The tissue sample was placed in a specially designed holder that coupled the two integrating spheres. The measurements were performed on the retinal and RPE-choroidal tissues at 514, 501, 488, and 476 nm from an argon ion laser (Spectra Physics model 2025). Although the maximum output power of the argon ion laser varied from 1 to 2 W, the average output power was kept at its minimum value of about 5 mW for all optical measurements. The laser beam diameter at $1/e^2$ was 1.25 mm and beam divergence was 0.70 mrad at 488 nm.

The schematic of the experimental setup for measuring the total diffuse reflectance and total diffuse transmittance is shown in Fig. 1. The experimental setup was similar to that used by Beek et al.[24] The laser beam was directed into the entrance port A of integrating sphere 1, whose exit port is coupled with the entrance port of integrating sphere 2; the sample was mounted at the coupling port C. The exit port B of integrating sphere 2 was covered with a cap with a reflective surface identical to that of the integrating spheres. The diameter of each sphere was 6 in. and each port had a diameter of

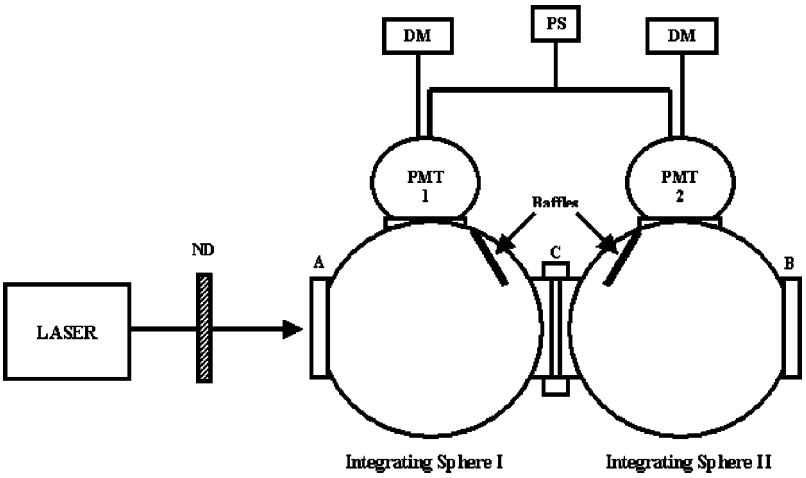

Fig. 1 Experimental setup for diffuse reflection and transmission measurements on bovine retinal and RPE-choroidal tissues. DM, digital multiplier; PS, power supply; PMT, photomultiplier tube; ND, neutral density filter.

1 in. Light leaving the sample reflected multiple times from the inner surfaces of the spheres before reaching the PMTs. Reflecting baffles within the spheres shielded the PMTs from the direct light from the sample. Port A was equipped with a variable aperture so that the beam diameter could be appropriately controlled. The reflected and transmitted light intensities were detected by two identical PMTs (Oriel model 77341); these were attached to the two measuring ports of integrating spheres 1 and 2. The PMTs were powered by a common power supply (Bertan model 215). The signals from the PMTs were measured by two identical Fluke digital multimeters (model 77 series II). The measured light intensities were then utilized to determine the total diffuse reflectance R_d and total diffuse transmittance T_d by the following expressions:

$$R_d = \frac{X_r - Y}{Z_r - Y} \tag{3}$$

and

$$T_d = \frac{X_t - Y}{Z_t - Y}, \tag{4}$$

where X_r is the reflected intensity detected by PMT-1 with the sample at C; Z_r is the incident intensity detected by PMT-1 without the sample at C and with the reflective surface at the exit port of integrating sphere 1; X_t is the transmitted intensity detected by PMT-2 with the sample at C; Z_t is the incident intensity detected by PMT-2 with no sample at C and with a reflective surface at B; and Y is the correction factor for the stray light measured by PMTs 1 and 2 with no sample at C or reflective surface at B.

2.5 *Measurement of Collimated Transmittance*

The unscattered collimated transmittance T_c was measured to determine the total attenuation coefficients. The collimated laser beam intensities were measured by placing an integrating sphere approximately 2 m behind the sample so that the photons scattered off the sample would not be able to enter the aperture of approximately 3 mm in diameter at the entrance port of the sphere. The sample was aligned at a right angle with respect to the incident beam. The collimated transmittance was calculated by the following relation:

$$T_c = \frac{X_c}{Z_c}, \tag{5}$$

where X_c is the collimated light intensity detected by a PMT (Oriel model 77341) attached to the measuring port of the integrating sphere and Z_c is the incident light intensity detected by the PMT with no sample in the light path; the reflective surface was placed at the exit port of the integrating sphere in both cases. Additional details on the experimental design can be found in Ref. 2.

2.6 *Inverse Adding Doubling Method*

In order to solve the radiative transport equation, the IAD algorithm[22] must be supplied with the experimentally deter-

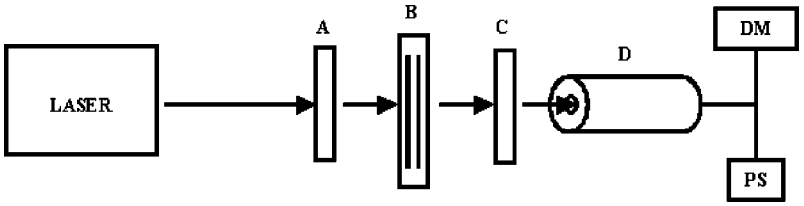

Fig. 2 Experimental setup for measuring polarization shifts in degrees on bovine retinal tissue. A, linear polarizer; B, sample; C, linear polarizer-analyzer; D, detector; PS, power supply; DM, digital multimeter.

Table 1 Polarization shift (in degrees) in bovine retinal and RPE-choroidal tissues from left and right eyes.

	Retina		RPE-Choroid	
Sample Number	Left	Right	Left	Right
1	5.96	6.96	10.92	12.16
2	5.92	4.92	10.00	11.94
3	6.94	5.00	11.96	13.92
Average	6.27	5.63	10.96	12.67

mined values of the total diffuse reflectance (R_d), total diffuse transmittance (T_d), and collimated transmittance (T_c). The IAD algorithm iteratively chooses the values for the dimensionless quantities: a and τ, defined in Eqs. (6) and (7), respectively, and then adjusts the value of the scattering anisotropy coefficient g until it matches the measured values of R_d and T_d:

$$a = \mu_s / (\mu_s + \mu_a) \tag{6}$$

and

$$\tau = t(\mu_s + \mu_a), \tag{7}$$

where μ_a and μ_s are the absorption coefficient and scattering coefficient, respectively and t is the physical thickness of the sample and is measured in centimeters. The values of a and τ provided by the IAD method are then used to calculate the absorption coefficient and scattering coefficient using Eqs. (6) and (7).

2.7 *Monte Carlo Simulation*

The accuracy of values of the absorption coefficient and scattering coefficient determined by the IAD method was verified by the MC simulation technique. This method uses a stochastic model to simulate light interaction in biological media. The μ_a and μ_s calculated by the IAD method, along with the experimentally determined index of refraction n and scattering anisotropy coefficient g were used to compute the R_d and T_d. These values were then compared for accuracy with the experimental values of R_d and T_d. A detailed theoretical description of the MC model in biological media is given by Prahl et al.[25]

Table 2 Polarization shift (in degrees) for combined retinal and RPE-choroidal tissues from the bovine left and right eyes.

	Retina and RPE-Choroid	
Sample Number	Left	Right
1	11.92	15.92
2	11.20	14.94
3	13.96	16.92
Average	12.36	15.93

Table 3 Polarization shift in the bovine right retina with time.

Time (h)	Polarization Shift (deg)
0	6.96
24	5.92
48	2.10

2.8 *Measurement of Polarization Shift*

The experimental setup for polarization measurements for retinal tissue is shown in Fig. 2. The He:Ne laser beam (Uniphase model 1101P) with a power of 4 mW and beam diameter of 3 mm was passed through a linear polarizer placed in front of the retinal sample position, beyond which was placed a second linear polarizer (analyzer). The polarizers were obtained from Oriel Corp. (Oriel model 25010). A photodiode detector that was provided with a low-bias voltage from a power supply (Cenco model 31382) was placed behind the analyzer; the photodiode was connected to a multimeter (Fluke model 77 series II). First, the polarizer (without the sample and analyzer in the laser path) was rotated until the maximum laser light intensity was obtained, indicating that the laser beam was completely polarized. Once the maximum laser intensity was achieved, the analyzer was placed behind a pair of blank slides (without the sample in the light path). The analyzer was then rotated to maximize the light intensity so that the transmission axes of the polarizer and analyzer were parallel. The reference condition was established with a pair of blank slides placed in the sample position. The blank slides were then replaced by the retinal sample placed between the polarizer and analyzer. The polarization shift of the scattered laser light was observed and the shift was determined by rotating the analyzer until maximum light intensity was achieved. Three retinal samples were prepared and measurements were taken at three different locations on each sample; the averages of the measurements on each sample are given in Tables 1 to 3.

The laser beam cannot penetrate RPE-choroidal tissue sample because of its opacity. Therefore, a simple modification of the experimental setup was made to measure the polarized light scattered off the RPE-choroidal tissue; it is shown in Fig. 3. A clean glass slide was placed in the sample holder and the scattered beam was directed at approximately a right angle with respect to the direction of the incident laser beam. The analyzer and photodiode were aligned with the direction of the most intense scattered beam. The same technique used for retinal tissue was employed to ensure that the transmission axes of both polarizer and analyzer were parallel. The glass slide was then replaced by the RPE-choroidal tissue sample. The polarization shift for the RPE-choroid was determined in the same manner as that for retinal tissue. For the RPE-choroidal sample, measurements were taken at three different locations on the sample; averages of the measure-

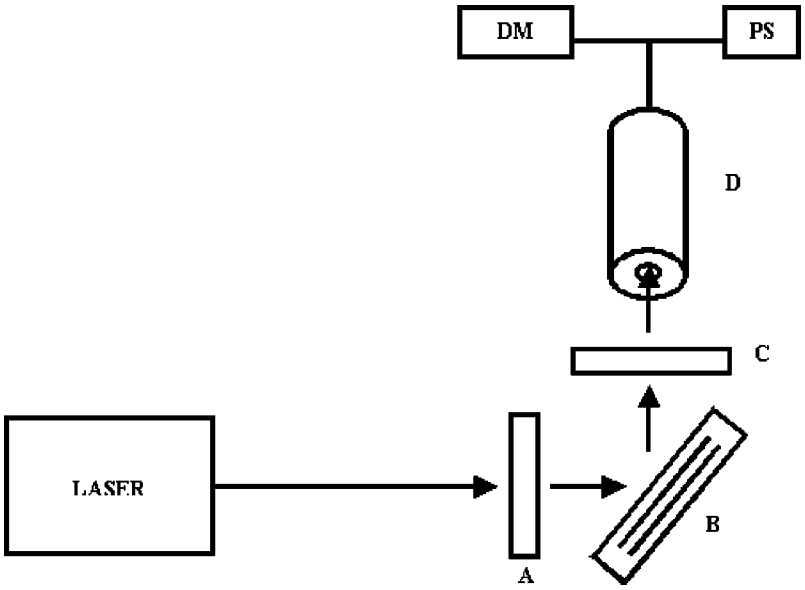

Fig. 3 Experimental setup for measuring polarization shifts in degrees on bovine RPE-choroidal tissue and a combination of retinal and RPE-choroidal tissues in a stack. A, linear polarizer; B, sample; C, linear polarizer-analyzer; D, detector; PS, power supply; DM, digital multimeter.

ments were calculated and are given in Tables 1 to 3. This was done to minimize the uncertainties in the measurements. The same experimental methodology was utilized for the polarization measurements on the retinal and RPE-choroidal tissues placed together. In this case, the retinal tissue sample was placed in front of the RPE-choroidal tissue sample.

3 Results and Discussion

The indices of refraction (n) of retinal and RPE-choroidal tissues varied from 1.34 to 1.38. The refractive indices of intact bovine retina are about 10% higher than those for melanin isolated from the bovine RPE melanosomes.[2] The measurements were repeated three times at each of the wavelengths used, and the values agreed to within 5%. The scattering anisotropy coefficients of retinal and RPE-choroidal tissues were determined to be between 0.92 and 0.96 from the goniometric measurements. For all of the IAD calculations, we used the average values of 1.36 and 0.94 for the index of refraction n and the scattering anisotropy coefficient g, respectively.

Total diffuse reflectance (R_d), total diffuse transmittance (T_d), and the collimated transmittance (T_c) values are given in Tables 4 and 5 for retinal and RPE-choroidal tissues, respectively. These measurements were repeated three times; the coefficient of variation of the measurements was determined to be approximately 4%. The margin of errors of the measurements of R_d, T_d, and T_c are also given in Tables 4 and 5. These values, along with the measured values of the index of refraction and the scattering anisotropy coefficient, were input into the IAD program. The output provided the dimensional quantities a and τ, defined by Eqs. (6) and (7), respectively. The absorption and scattering coefficients were

Table 4 Wavelength-dependent absorption coefficient (μ_a), scattering coefficient (μ_s), total attenuation coefficient (μ_t), mean-free-path ($1/\mu_t$), albedo (a), and optical depth (τ) as determined by IAD using the measured diffuse reflectance (R_d), diffuse transmittance (T_d), and collimated transmittance (T_c) for bovine retina. The margin of error is given below the measured values.

	Experimental			IAD					
Wavelength (nm)	R_d	T_d	T_c	a	τ	μ_a (cm^{-1})	μ_s (cm^{-1})	μ_t (cm^{-1})	$1/\mu_t$ (cm)
514	0.061 ±0.005	0.79 ±0.06	0.110 ±0.008	0.952	2.16	10.4	205	215.4	0.004645
501	0.060 ±0.004	0.76 ±0.06	0.112 ±0.008	0.939	2.15	13.0	202	215.0	0.00465
488	0.058 ±0.004	0.70 ±0.05	0.112 ±0.008	0.915	2.14	18.2	196	214.2	0.00467
476	0.054 ±0.004	0.65 ±0.05	0.131 ±0.010	0.882	1.99	23.5	175	198.5	0.00504

Table 5 Wavelength-dependent absorption coefficient (μ_a), scattering coefficient (μ_s), total attenuation coefficient (μ_t), mean-free-path ($1/\mu_t$), albedo (a), and optical depth (τ) as determined by IAD using the measured diffuse reflectance (R_d), diffuse transmittance (T_d), and collimated transmittance (T_c) for bovine RPE-choroid. The margin of error is given below the measured values.

	Experimental			IAD					
Wavelength (nm)	R_d	T_d	T_c	a	τ	μ_a (cm^{-1})	μ_s (cm^{-1})	μ_t (cm^{-1})	$1/\mu_t$ (cm)
514	0.1454 ±0.011	0.00050 ±0.00004	0.00030 ±0.00002	0.545	8.06	245	293	538	0.00186
501	0.1877 ±0.014	0.00050 ±0.00004	0.00040 ±0.00003	0.422	7.78	300	219	519	0.00193
488	0.0887 ±0.007	0.00060 ±0.00004	0.00050 ±0.00004	0.344	7.55	330	173	503	0.00199
476	0.1244 ±0.009	0.00140 ±0.00010	0.00100 ±0.00007	0.630	7.55	238	219	457	0.00219

then calculated from the values of a and τ. The absorption coefficient, scattering coefficient, total attenuation coefficient ($\mu_t = \mu_a + \mu_s$), penetration depth ($1/\mu_t$), albedo (a), and optical depth (τ) for the retinal and RPE-choroidal tissues are given in Tables 4 and 5, respectively. The measured values of R_d and T_d used to calculate μ_a and μ_s by the IAD method were compared with those generated by the MC simulation technique. These values are given in Tables 6 and 7 for retinal and RPE-choroidal tissue, respectively.

In retinal tissue, the scattering was found to be significantly higher than the absorption, while in the RPE-choroidal tissue, both the absorption and scattering were found to be comparable. However, the total attenuation coefficients of the RPE-choroid are consistently higher than those of the retina. This is perhaps because the RPE-choroid is physiologically more opaque and contains melanin. The values of the attenuation coefficients of the retina can be attributed to some inadvertant cross-contamination of the retina with melanin granules from the RPE during sample preparation. Since the attenuation coefficients of RPE-choroidal tissue at all wavelengths investigated are significantly higher than those of the retina, the penetration depths in the RPE-choroid are much smaller than those in the retina. The actual values of the absorption and scattering coefficients for the retinal and RPE-choroidal tissues reported in this study have importance for practical applications requiring the prediction of light transport through pigmented tissue, e.g., in the design of treatment models for laser-induced thermotherapy or photodynamic therapy in the eye, where the degree of pigmentation at the target sites may vary. Variable pigmentation obviously complicates the laser dosimetry for such treatment modes because the amount of light delivered will have to be adjusted for the amount of tissue pigmentation in order to achieve some standard clinical effect.[2]

The data for the shifts of polarization in the retinal and RPE-choroidal tissues are given in Tables 1 and 2. The experimental data were tested for normality with a statistical software program, SPSS; the data exhibited normal distribution. At this point, a basic student's *t*-test was performed on the samples. With an alpha level of 0.05, a comparison of the polarization shifts between the left and right eye samples yielded a *t*-value of 3.55. Since this is larger than the accepted *t*-value of 2.78 (at 0.05 alpha level), the difference is statistically significant. The variations observed in the polarization shifts between the left and right eyes could be due to minuscule differences in thickness in the prepared tissue samples, particularly when different spots on the same sample were chosen for collecting the data. Our data clearly suggest that the bovine ocular tissues possess strong polarization properties. However, the RPE-choroidal tissue shows a higher de-

Table 6 Wavelength-dependent diffuse reflectance (R_d) and diffuse transmittance (T_d) determined by the experimental and Monte Carlo techniques for bovine retina.

	Experimental		Monte Carlo		Percent Difference	
Wavelength (nm)	R_d	T_d	R_d	T_d	R_d	T_d
514	0.0614	0.7862	0.0673	0.7606	8.78	3.36
501	0.0598	0.7580	0.0608	0.7404	1.57	2.38
488	0.058	0.7008	0.0539	0.6979	7.70	0.42
476	0.0544	0.6531	0.0545	0.6587	0.27	0.85

Table 7 Wavelength-dependent diffuse reflectance (R_d) and diffuse transmittance (T_d), determined by the experimental and Monte Carlo techniques for bovine RPE/choroid.

Wavelength (nm)	Experimental		Monte Carlo		Percent Difference	
	R_d	T_d	R_d	T_d	R_d	T_d
514	0.1454	0.0005	0.1400	0.00053	3.89	5.03
501	0.1877	0.0005	0.1728	0.00052	8.65	4.10
488	0.0887	0.0006	0.0839	0.00064	5.75	6.54
476	0.1244	0.0014	0.1179	0.00150	5.52	6.95

gree of polarization shift than the retina. We also measured the polarization shifts in the bovine retina at 24-h intervals and found that the shift decreases significantly 48 h after sample preparation. These values are given in Table 3. During this period of measurement, the samples were kept refrigerated. The sharp decrease in polarization shift can be attributed to the physiological degradation of the retinal tissue, which changed the optical properties drastically.

Retinal neovascularization resulting from diabetic retinopathy is the most common cause of blindness in young patients in major industrialized countries,[26,27] and choroidal neovascularization resulting from age-related macular degeneration is the most common cause of severe vision loss in elderly patients.[28] This retinal vascular development occurs by a combination of vasculogenesis and angiogenesis.[29,30] An additional diagnostic application of retinal polarization would be to evaluate the effect of glaucomatous damage to the nerve fiber layer in the retina. This is based on an excellent study by Ducros et al.,[31] who have reported that polarization-sensitive optical coherence tomography (PSOCT) can determine the thickness and birefringence of the retinal nerve fiber layer.

High transmittance values in the visible region have been reported in previous studies on retinal and RPE-choroidal tissues.[32,33] Geeraets and Berry[32] found that in the visible region transmittance was greater than 80% in human, rabbit, and monkey retinal tissues. However, Van den Berg and Spekreijse[33] argued that the data presented by Boettner and Wolter[34] could be explained only on the basis of pure water content in the ocular tissues. Additional studies on the spectral properties of ocular media ranging from UV through near-infrared have been reported by other authors.[35–39] The high transmittance and very low reflectance values in the visible region reported by these authors are similar to ours.

The optical polarization studies presented in this article show that the bovine retina and RPE-choroid both possess strong polarization characteristics. It was shown earlier that the light-scattering property of biological tissues can be used as a diagnostic tool.[4] In addition, owing to retinal and subretinal birefringence characteristics, an optical polarization study of ocular tissues is important for noninvasive diagnosis of neovascularized tissues. Therefore, further polarimetry investigations of retinal and RPE-choroidal tissues, especially from human eyes at different pathological stages are imperative for the development of a quantitative, noninvasive diagnostic technique for ocular diseases.

Acknowledgments

This work was supported in part by the a University of Texas at San Antonio Faculty Development Award to one of the authors (DKS). The authors would like to thank Elia Villazana for preparing all the bovine tissue samples used in this study. The authors would also like to thank Scott Prahl (Oregon Medical Laser Center) for the use of the inverse adding doubling source code and Steven L. Jacques (Oregon Medical Laser Center) and Lihong Wang (Texas A&M University) for the use of the source code for the Monte Carlo model. Support by the National Science Foundation-sponsored CBST at the University of California Davis is gratefully acknowledged.

References

1. T. Sarna, ''Properties and function of the ocular melanin—a photobiophysical view,'' *Photochem. Photobiol.* **12**, 215–258 (1992).
2. D. K. Sardar, M. L. Mayo, and R. D. Glickman, ''Optical characterization of melanin,'' *J. Biomed. Opt.* **6**, 404–411 (2001).
3. T. P. Dryja, M. O'Neil-Dryja, and D. M. Albert, ''Elemental analysis of melanins from bovine hair, iris, choroid, and retinal pigment epithelium,'' *Invest. Ophthalmol. Vis. Sci.* **18**, 231–236 (1979).
4. J. R. Mourant, A. H. Hielscher, J. P. Freyer, and A. A. Eick, ''Scattering properties of biological cells,'' *Biomed. Opt. Spectrosc. Diagnostics, OSA TOPS*, **22**, 11–14 (1998).
5. D. K. Sardar and L. B. Levy, ''Optical properties of whole blood,'' *Lasers Med. Sci.* **13**, 106–111 (1998).
6. S. Chandrasekhar, *Radiative Transfer*, Dover, New York (1960).
7. P. Kubelka, ''New contributions to the optics of intensely light-scattering materials,'' *J. Opt. Soc. Am.* **38**, 448–457 (1948).
8. F. Kottler, ''Turbid media with plane-parallel surfaces,'' *J. Opt. Soc. Am.* **50**, 483–490 (1960).
9. S. Wan, R. R. Anderson, and J. A. Parish, ''Analytical modeling for the optical properties of the skin with in vitro and in vivo applications,'' *Photochem. Photobiol.* **34**, 493–499 (1981).
10. R. R. Anderson and J. J. Parish, ''The optics of human skin,'' *J. Invest. Dermatol.* **77**, 13–19 (1981).
11. S. Ertefai and A. E. Profio, ''Spectral transmittance and contrast in breast diaphanography,'' *Med. Phys.* **12**, 393–400 (1985).
12. M. J. C. van Gemert, R. Verdaasdonk, E. G. Stassen, G. A. C. M. Schets, G. H. M. Gijsbers, and J. J. Bonnier, ''Optical properties of human blood vessel wall and plaque,'' *Lasers Surg. Med.* **5**, 235–237 (1985).
13. M. R. Prince, F. T. Deutsch, R. Margolis, M. M. Mathews-Roth, J. A. Parrish, and A. S. Oseroff, ''Preferential light absorption in atheromas: implication for laser angioplasty,'' *J. Clin. Invest.* **78**, 295–302 (1978).
14. A. Ishimaru, *Wave Propagation and Scattering in Random Media*, Vol. 1, Academic Press, New York (1978).
15. L. Reynolds, C. C. Johnson, and A. Ishimaru, ''Diffuse reflectance from a finite blood medium: application to the modeling of fiberoptic catheters,'' *Appl. Opt.* **15**, 2059–2067 (1978).

16. R. A. J. Groenhuis, H. A. Ferwerda, and J. J. Ten Bosch, ''Scattering and absorption of turbid materials determined from reflection measurements. 1: Theory,'' *Appl. Opt.* **22**, 2456–2462 (1983).
17. M. J. C. van Gemert, A. J. Welch, W. M. Star, and M. Motamedi, ''Tissue optics for a slab geometry in diffusion approximation,'' *Lasers Med. Sci.* **2**, 295–302 (1987) and references therein.
18. M. J. C. van Gemert and W. M. Star, ''Relations between the Kubelka-Munk and transport equation models for anisotropic scattering,'' *Lasers Life Sci.* **1**, 287–298 (1987).
19. J. Hourdakis and A. Perris, ''A Monte Carlo estimation of tissue optical properties for use in laser dosimetry,'' *Phys. Med. Biol.* **40**, 351–364 (1995).
20. M. Hammer, A. Roggan, D. Schweitzer, and G. Muller, ''Optical properties of ocular tissues, an in vitro study using the double-integrating-sphere technique and inverse Monte Carlo simulation,'' *Phys. Med. Biol.* **40**, 963–977 (1995).
21. S. L. Jacques and L. Wang, ''Monte Carlo modeling of light transport in tissues,'' in *Optical-Thermal Response of Laser-Irradiated Tissue*, A. J. Welch and M. J. C. van Gemert, Eds. Plenum, New York and London (1995).
22. S. A. Prahl, M. J. C. Van Gemert, and A. J. Welch, ''Determining the optical properties of turbid media by using the inverse adding-doubling method,'' *Appl. Opt.* **32**, 559–568 (1993).
23. E. Hecht, Optics, 4th ed., Addison Wesley, New York (2002).
24. J. F. Beek, H. J. Staveren, P. Posthumus, H. J. C. M. Sternborg, and M. J. C. van Gemert, ''In vitro double-integrating-sphere optical properties of tissue between 630 and 1064 nm,'' *Phys. Med. Biol.* **42**, 2255–2261 (1997).
25. S. A. Prahl, M. Keijzer, S. L. Jacques, and A. J. Welch, ''A Monte Carlo model of light propagation in tissue,'' SPIE Institute Series **IS 5**, 102–111 (1989).
26. H. Kahn and R. Hiller, ''Blindness caused by diabetic retinopathy,'' *Am. J. Ophthalmol.* **78**, 58–67 (1974).
27. R. Klein and B. Klein, ''Vision disorders in diabetes,'' in *Diabetes in America*, p. 294, National Institutes of Health, Washington, DC (1995).
28. P. A. Campochiaro, ''Retinal and choroidal neovascularization,'' *J. Cell Physiol.* **184**, 301–310 (2000).
29. J. R. McLeod, G. A. Lutty, and R. W. Wajer, ''Visualization of developing vasculature,'' *Microvasc. Res.* **33**, 257–269 (1987).
30. J. R. McLeod, S. N. Crone, and G. A. Lutty, ''Visoproliferation in the neonatal dog model of oxygen-induced retinopathy,'' *Invest. Ophthalmol. Visual Sci.* **37**, 1322–1333 (1996).
31. M. G. Ducros, J. D. Marsack, H. G. Rylander III, and S. L. Thomson, ''Primate retina imaging with polarization-sensitive optical coherence tomography,'' *J. Opt. Soc. Am. A* **18**, 2945–2956 (2001).
32. W. J. Geeraets and E. R. Berry, ''Ocular spectral characteristics as related to hazards from lasers and other light sources,'' *Am. J. Ophthalmol* **66**, 15–20 (1968).
33. T. J. T. P. van den Berg and H. Spekreijse, ''Near infrared light absorption in the human eye media,'' *Vision Res.* **37**, 249–253 (1997).
34. E. A. Boettner and J. R. Wolter, ''Transmission of the ocular media,'' *Invest. Ophthalmol.* **1**, 777–783 (1962).
35. F. C. Delori and K. P. Pflibsen, ''Spectral reflectance of the human ocular fundus,'' *Appl. Opt.* **28**(6), 1061–1077 (1989).
36. R. W. Knighton, S. G. Jacobson, and C. M. Kemp, ''The spectral reflectance of the nerve fiber layer of the macaque retina,'' *Invest. Ophthalmol. Visual Sci.* **30**(11), 2393–2402 (1989).
37. J. J. Vos, A. A. Munnik, and J. Boogaard, ''Absolute spectral reflectance of the fundus oculi,'' *J. Opt. Soc. Am.* **55**, 573–574 (1965).
38. R. W. Fowler, D. S. McLeod, and S. M. Pitts, ''The effect of blood on ocular fundus reflectance and determination of some optical properties of retinal blood vessels,'' *Invest. Ophthalmol. Visual Sci.* **17**(6), 562–565 (1978).
39. E. F. Maher, ''Transmission and absorption coefficients for ocular media of the rhesus monkey,'' USAF School of Aerospace Med., Brooks AF Base, TX, Report SAM-TR-78-32 (1978).